Experimental investigation of heterogeneous mechanical tests

GONÇALVES Mafalda[1,a *], GUEGAN Briag[2,b], THUILLIER Sandrine[2,c] and ANDRADE-CAMPOS António[1,d]

[1]Department of Mechanical Engineering, TEMA - Centre for Mechanical Technology and Automation, LASI - Intelligent Systems Associate Laboratory, University of Aveiro, Campus Universitario de Santiago, 3810-193 Aveiro, Portugal

[2]Univ. Bretagne Sud, UMR CNRS 6027, IRDL, F-56100 Lorient, France

[a]mafalda.goncalves@ua.pt, [b]briag.guegan@grenoble-inp.org, [c]sandrine.thuillier@univ-ubs.fr, [d]gilac@ua.pt

Keywords: Heterogeneous Test, Digital Image Correlation, Mechanical Behavior, Sheet Metal

Abstract. The virtualization of sheet metal forming processes requires a precise numerical model with an accurate description of the material behavior that is classically obtained by carrying out quasi-homogeneous mechanical tests. However, several alternatives to this time-consuming task are under study. Heterogeneous tests can provide a large quantity of mechanical information in a single experiment and, therefore, their potential needs to be investigated. This work aims to present an advanced mechanical test designed by topology optimization under experimental investigation. A numerical design methodology is described, leading to a specimen geometry that is subjected experimentally to uniaxial tensile loading up to rupture. A dual-phase DP600 steel is used. During the test, the strain field is extracted from the specimen surface using a stereo digital image correlation system, and the richness of the mechanical information is further analyzed.

Introduction

Numerical simulation has played a major role in the virtualization of sheet metal forming processes. This process leads to a reduced number of issues or failed processes, resulting in a reduction in cost, material waste, and development time of sheet metal forming parts. However, it requires an accurate numerical model, which in turn relies on an exact representation of the material mechanical behavior. This is only possible with an adequate constitutive model that is accurately calibrated, providing a good agreement between the real material behavior and the one predicted by the model equations. Therefore, model calibration procedures play a key role in the process.

Quasi-homogeneous mechanical tests are classically performed to obtain the required information to characterize material behavior; however, a large number of different tests are required to cover a wide range of strain and stress states. Heterogeneous mechanical tests are being used to reduce the experimental effort and speed up the model calibration and, therefore, the material behavior characterization task. The more complex boundary conditions and/or geometries can give them the ability to provide a larger variety of strain and stress states in a single experiment. To replace classical methods, full-field measurement techniques such as Digital Image Correlation (DIC) and inverse identification techniques are being used side by side with advanced mechanical tests to exploit their full potential [1]. These new techniques have been referred to as Material Testing 2.0 [2].

Several works have already addressed the calibration of material models using inverse methods with full-field data from heterogeneous mechanical tests [3-11]. However, it is important to note that some of these works remain on the use of numerical data from virtual tests. As for actual experiments, for example, Zhang et al. [9] used the heterogeneous strain field of a biaxial test to calibrate an advanced anisotropic yield function for an aluminum alloy and a dual-phase steel. Lou et al. [10] calibrated a yield function and a hardening law using designed specimens via an inverse experimental-numerical procedure. Aquino et al. [11] used a mechanical test designed by shape optimization to calibrate a yield criterion via a Finite Element Model Updating (FEMU) strategy.

To fill this gap and to experimentally investigate the potential of these new procedures, this work aims at designing an original mechanical test using topology optimization and validating its design experimentally. The design procedure attempts to increase the strain heterogeneities in the specimen by maximizing the heterogeneity of the displacement field. The optimal specimen geometry is experimentally subjected to a uniaxial tensile loading up to rupture. The mechanical information is extracted from the specimen surface using full-field measurements and evaluated to analyze the relevance of the test for improving model calibration procedures. The paper is split into three main parts, dedicated to the test design procedure, then to the experiments using the optimized geometry and a dual phase steel and finally to an analysis of the results.

Test design procedure

Framework. The design of mechanical tests has been addressed in several works, trying to obtain a mechanical test from which a large variety of strain and stress states can be retrieved to improve model calibration. The use of optimization techniques in the design procedure has shown improved efficiency and quality of the solutions [12]. In this work, the test design procedure applies topology optimization to the design of compliant mechanisms [13]. While the former is a design method that aims to find the best material distribution for a design domain, the latter is known for deforming its flexible members as a consequence of the applied displacement. The main idea is to gather the potential of topology optimization to generate non-standard specimen geometries with heterogeneous displacement fields and the possibility of enhancing such heterogeneity by controlling the displacements in specific locations of the specimen according to the compliant mechanisms' theory. Depending on the applied displacements, specific strain/stress states can be induced on the specimen. Such heterogeneity of strain/stress states can lead to richer mechanical tests that will improve the accuracy and efficiency of model calibration procedures due to the high diversity of mechanical information.

In this work, the test design starts from a design domain shown in Figure 1. While a uniaxial tensile loading test is reproduced, the aim is to find the optimal material distribution that maximizes the displacement field heterogeneity. The load applied by the grips of the testing machine is represented by $\mathbf{F}_{\text{in}}$. To control the displacement field, two displacements are applied in different directions and locations of the specimen to impose different deformation states. To provide stiffness to the solution, $\mathbf{u}_{\text{in}}$, corresponds to the displacement of the grips during the test. The location and direction of the displacement $\mathbf{u}_{\text{out}}$ determine the way the specimen behaves. To avoid numerical issues during the design optimization, two springs of stiffness, K_{in} and K_{out}, are implemented at the input and output locations, respectively. The design optimization is only performed in one quarter of the test geometry since double symmetry conditions are assumed.

Problem formulation. The design domain can be described by topology optimization as a finite element mesh. Each element is represented by a design variable, X_e, that corresponds to the element's relative density. Depending on the quantity of material, it can assume values between 0 and 1 if the element is respectively void or full of material. At the beginning, 35% of the total material is associated to each element ($\mathrm{X_e} = 0.35,\ e = 1, \ldots, M$ and M the total number of elements). During the optimization, according to the objective-function evolution, material is added or removed from each element in order to find the optimum material layout. The material distribution is here represented by **X.**

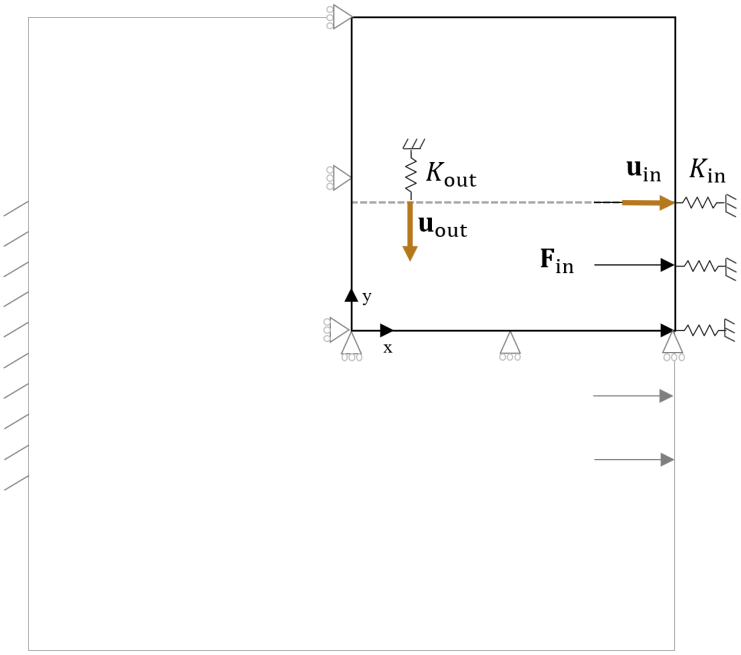

Fig. 1. Schematic representation of the test design domain subjected to a uniaxial tensile loading. Double symmetry conditions are assumed and only a quarter of the specimen is optimized.

It is proposed to find the specimen geometry (material distribution) that presents the most heterogeneous displacement field. While the input displacement gives stiffness to the solution, the output displacement is responsible for creating heterogeneity. Therefore, to increase the potential of the specimen, it is proposed to maximize the ratio between the output and input displacements. The problem formulation is here represented:

$$\begin{aligned} \underset{\mathbf{X}}{\text{maximize}} \quad & T(\mathbf{X}) = \frac{u_{\text{out}}(\mathbf{X})}{u_{\text{in}}(\mathbf{X})}, \\ \text{subject to} \quad & \mathbf{R} = \mathbf{0}, \\ & \frac{\sum_{e=1}^{M} X_e V_e}{\sum_{e=1}^{M} V_e} - V^* \leq 0, \\ & 0 \leq \rho_{\min} \leq X_e \leq 1, e = 1,2,\dots,M. \end{aligned} \tag{1}$$

The optimization problem is solved by taking into account three constraints: system equilibrium, design domain volume fraction and the limits of the design variables. The first one requires solving a nonlinear finite element analysis at each iteration until the equilibrium between the internal and external loads is achieved ($\mathbf{R} = 0$) [14]. Nonlinear geometric and material nonlinearities are considered in the design procedure. The volume constraint establishes a limit for the maximum volume fraction of the design domain, V^*, meaning the sum of each element's volume fraction, V_e. For each element, a lower limit for the relative density, ρ_{min}, is imposed to avoid numerical issues.

Obtained geometry. Based on a previous work [13], the initial configuration of the design domain as well as the volume fraction were established. A mesh of 50x50 elements is used to discretize the design domain and a volume fraction of 35% is imposed. While the input displacement corresponds to the displacement of the grips, the output displacement is applied in the left symmetry boundary pointing downwards. The elastic and Swift's hardening law parameters presented in Table 1 were used to reproduce the elastoplastic material behavior.

Table 1. Elastic and Swift hardening law parameters for a DP600 steel.

Elastic		Swift hardening law		
E [GPa]	v [-]	K [MPa]	ε_0 [-]	n [-]
210	0.3	979.46	0.00535	0.194

As mentioned, the optimization process starts from a uniform material distribution, in which each element presents the same material quantity. From then on, depending on the objective-function evolution, the material is distributed according to the necessity of each element, leading to a final material layout. The evolution of the material layout, from the initial design domain until the final configuration, is represented in Figure 2. Only one quarter of the specimen is represented in five of the 37 iterations of the optimization process.

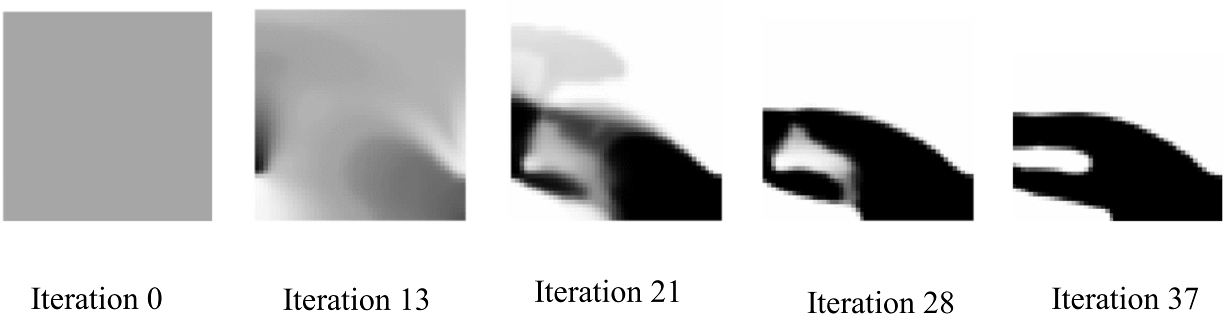

Fig. 2. Evolution of the material layout of one quarter of the specimen since the initial design domain (iteration 1) until the final material layout (iteration 37).

Although only one quarter is obtained, double symmetry is assumed and, therefore, the numerical design obtained by a topology optimization design procedure, referred to as TopOpt, is represented in Figure 3. From the numerical design, a smoothing of the specimen boundaries was made due to machining requirements and, therefore, an approximation of the original shapes was made. The height of the grips must be 40 cm and, therefore, the specimen was scaled, maintaining the ratio between the width and height of the specimen. The dimensions of the final configuration of the specimen are presented in Figure 4 and more details can be found in [15]. This geometry was investigated numerically in [15] alongside other advanced mechanical tests, in which their potential to improve model calibration procedures was analyzed.

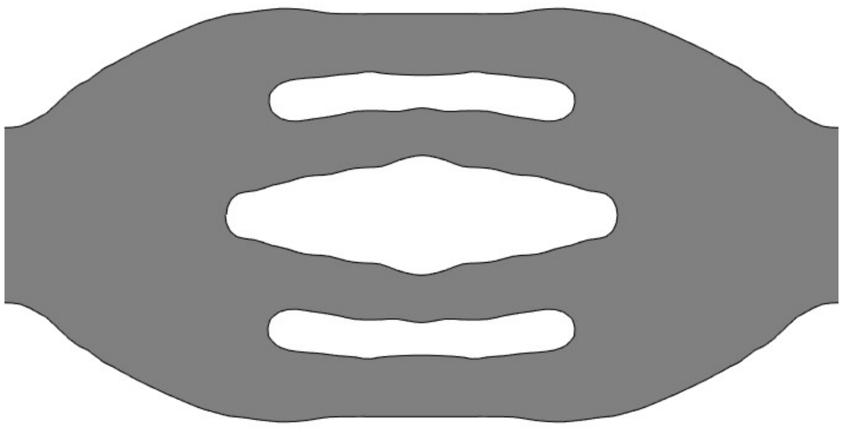

Fig. 3. Numerical design obtained by a topology optimization design procedure.

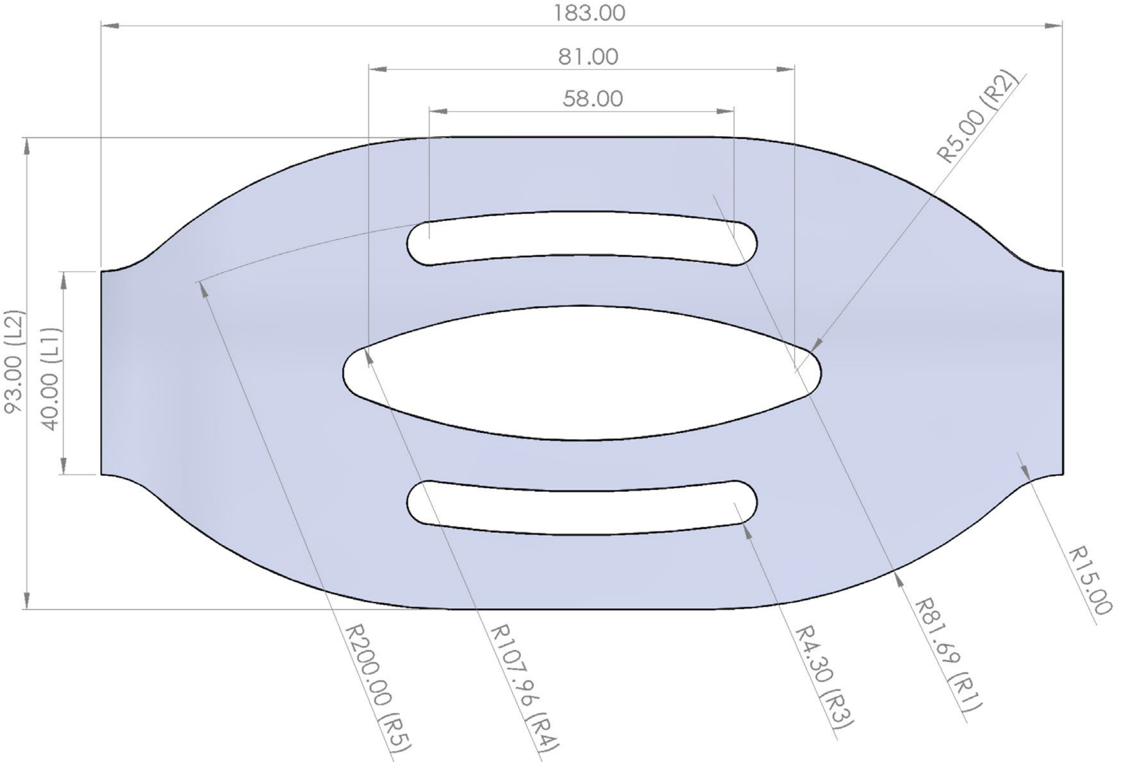

Fig. 4. TopOpt specimen geometry and general dimensions in mm.

Experimental procedure

Specimen design. For the experimental procedure, the specimen depicted in Figure 4 was used. A rectangular section of 55 cm length was added to each side of the geometry for the grips. Specimens are cut by water jet and the Y axis of the specimen frame is inclined at 45º with respect to the rolling direction. Due to the inaccuracy of the cutting technique, some measured dimensions are not strictly equal to the theoretical ones. The theoretical and measured dimensions as well as the deviation between them are presented in Table 2.

Table 2. Theoretical and measured dimensions as well as the deviation between them.

	L1	L2	R1	R2	R3	R4	R5	t
Theoretical [mm]	40	93	81.69	5	4.30	107.96	200	0.80
Measured [mm]	39.95	88.07	78.02	4.90	4.22	102.15	189.62	0.81
Deviation [%]	0.13	5.30	4.49	2	1.86	5.38	5.19	1.25

Material. The material investigated in this work is a dual-phase DP600 steel of thickness 0.8 mm. The mechanical properties of the material, measured with tensile tests at several orientations to the rolling direction, are given in Table 3 such as the ultimate yield stress, R_m, and the average and standard deviation of the plastic anisotropy coefficients, $\overline{r}$ and Δr, respectively.

Table 3. Mechanical properties of DP600 steel.

$\boldsymbol{R_\mathrm{m}}$ **[MPa]**	$\boldsymbol{\overline{r}}$	$\boldsymbol{\Delta r}$
661.9	0.999	0.085

Test and DIC setup. The specimen geometries are submitted to a uniaxial tensile loading, using an Instron 5969 machine equipped with a load cell of 50 kN maximum capacity. The specimen is clamped on both sides and a test speed of 3 mm/min is set.

To measure the deformation from the specimen surface during the test, Digital Image Correlation is used as a full-field measurement technique. The optical measurement technique requires the application of a random speckle pattern on the specimen surface that follows the deformation of the test. In this work, a spray-painting technique was used consisting in a mate white coat uniformly distributed and a layer of random black dots. Throughout the test, by taking and correlating two consecutive pictures of the specimen, it is possible to obtain the displacement and strain fields. The experimental acquisition was made with the commercial software VIC 3D developed by Correlated Solutions. In order to improve the accuracy of the results by taking advantage of the potential of the cameras sensor, the two cameras were placed vertically. The following analysis to compute the mechanical fields was performed with MatchID. The hardware configuration and the DIC analysis settings are presented in Table 4. More details on the full-field measurement technique can be found in [15].

Results

Due to the complex geometry of the specimen, a buckling phenomenon is noticed during the test leading to an out-of-plane behavior. The buckling effect starts to be non-negligible after a grips' displacement of 1 mm where the out-of-plane displacement is almost 4 mm. At the moment just before rupture, after 18.43 mm of displacement of the grips, the specimen configuration is represented in Figure 5. This behavior, associated with plastic buckling, was observed in all tests performed, making this test repeatable and suitable for material testing.

Table 4. DIC system configuration and analysis' settings.

	TopOpt
Camera 0 (noise)	Basler ac A2440-35um 5MP (0.71%)
Image resolution	2048 x 2448
Camera 1 (noise)	Basler ac A2440-35um 5MP (0.75%)
Image resolution	2048 x 2448
Focal length	35 µm
Stereo angle	25
FOV [mm]	173.6 x 207.3
Distance [mm]	860
Correlation algorithm	ZNSSD
Interpolation	Local bicubic splines
Subset shape function	Quadratic
Subset and step size	19/8
Image prefiltering	Gaussian
Strain window and convention	7/Log. Euler-Almansi
Progress history	Spatial + Update reference
Noise floor (displacement and strain)	1.44 x 10^{-3}, 1.36 x 10^{-4}

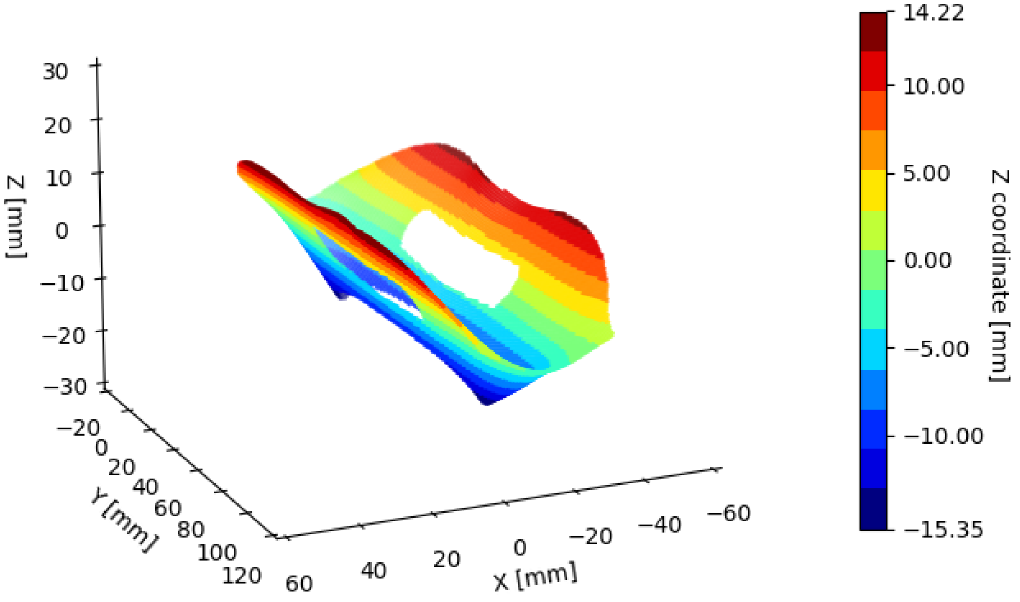

Fig. 5. Final configuration of the specimen at the moment just before rupture. The colormap represents the Z-coordinate over the specimen, highlighting the out-of-plane behavior of the test.

Due to this behavior, the mechanical information presented by one surface is different from the other. Therefore, a larger variety of information than the one presented by one surface can be extracted from a single experiment. The mechanical test was performed with two similar DIC setups, one of each side of the specimen, to be possible to extract all the information that can be provided by the specimen. Therefore, Figure 6 represents the principal maximum and minimum strain fields on the specimen surfaces (from DIC systems 1 and 2) just before rupture.

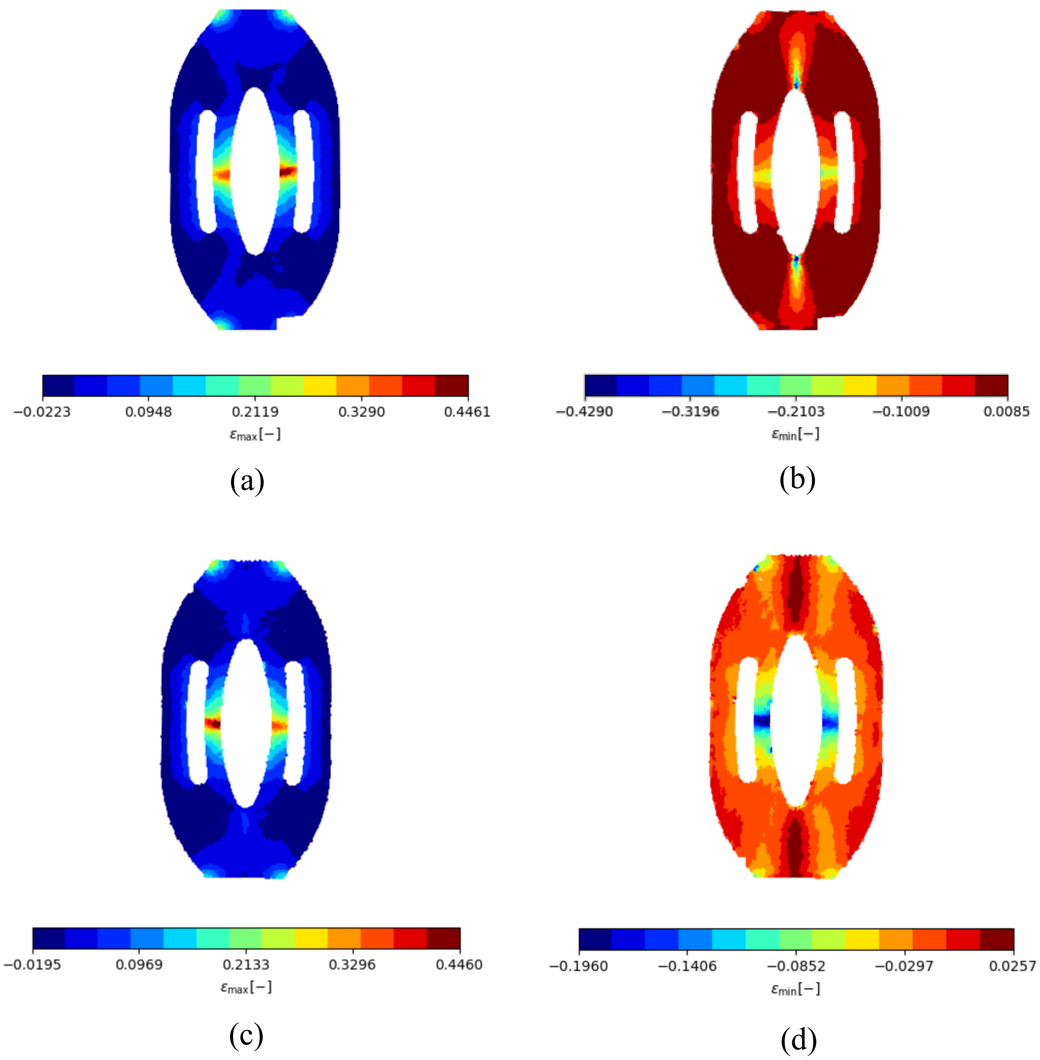

(a) (b)

(c) (d)

Fig. 6. Experimental principal maximum and minimum strain fields on the specimen surfaces from DIC systems 2: (a) and (b) and 1: (c) and (d).

It can be noted that high strain magnitude values are achieved, however the peak values are very localized and near the specimen boundaries. The peak values may be missed by the measurement technique due to their location and weakness of DIC of extracting information close to the edges. Moreover, some data was not possible to be read by system 2 causing the white area on the bottom corner of Figures 6 (a) and (c).

The main purpose of the test is to provide a large variety of strain states due to the heterogeneities present in the strain field. The strain state heterogeneity on the specimen can be better investigated by analyzing the principal strain diagram that is represented in Figure 7. The information provided by both DIC systems is represented. It is worth noting that, in addition to the points in uniaxial tension, an interesting quantity of material points are placed between uniaxial and plane strain compression. Moreover, even with lower strain magnitudes, some material points are under shear and uniaxial compression. To level the information provided by this heterogeneous mechanical test, several quasi-homogeneous mechanical tests would have to be performed, supporting the works dedicated to Material Testing 2.0.

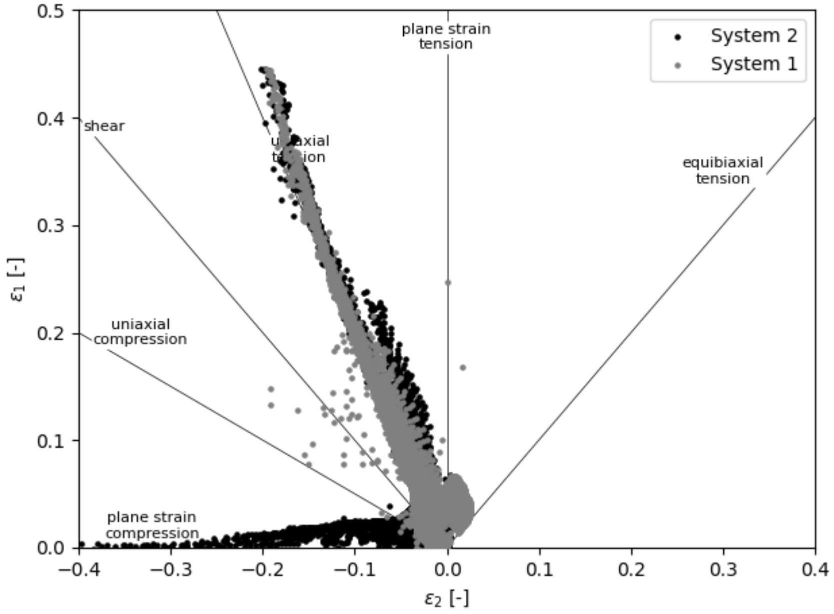

Fig. 7. Principal strain diagram with information from DIC systems 1 and 2 just before fracture.

Concluding remarks

This work addressed the numerical design of a mechanical test using topology optimization as a design method and its validation through mechanical experiments. With the aim of covering a wide range of strain and stress states, a specimen geometry was obtained presenting a high heterogeneous displacement field. This specimen was subjected experimentally to uniaxial tensile loading up to rupture. Two Digital Image Correlation systems were used to extract the full-field information from the specimen surfaces during the test. A large range of strain states was recorded on the specimen surfaces, overcoming the ones presented by standard and quasi-homogeneous mechanical tests.

Acknowledgments. This project has received funding from the Research Fund for Coal and Steel under grant agreement No 888153. This paper was also supported by the projects UIDB/00481/2020 and UIDP/00481/2020 - Fundação para a Ciência e a Tecnologia, DOI 10.54499/UIDB/00481/2020 and DOI 10.54499/UIDP/00481/2020. M. Gonçalves is grateful to the FCT for the Ph.D. grant Ref. UI/BD/151257/2021 and to the ESAFORM association for the mobility grant.

References

[1] J.M.P. Martins, S. Thuillier, A. Andrade-Campos, Calibration of a modified Johnson-Cook model using the Virtual Fields Method and a heterogeneous thermo-mechanical tensile test, Int J Mech Sci 106511 (2021) 202-203. https://doi.org/10.1016/j.ijmecsci.2021.106511

[2] F. Pierron, M. Grédiac, Towards Material Testing 2.0. A review of test design for identification of constitutive parameters from full-field measurements, Strain 57 (2021) 1–22. https://doi.org/10.1111/str.12370

[3] Y. Zhang, S. Gothivarekar, M. Conde, A. Van de Velde, B. Paermentier, A. Andrade-Campos, et al. Enhancing the information-richness of sheet metal specimens for inverse identification of

plastic anisotropy through strain fields, Int J Mech Sci 214 (2022) 106891. https://doi.org/10.1016/j.ijmecsci.2021.106891

[4] M. Conde, Y. Zhang, J. Henriques, S. Coppieters, A. Andrade-Campos. Design and validation of a heterogeneous interior notched specimen for inverse material parameter identification, Finite Elem Anal Des 214 (2023) 103866. https://doi.org/10.1016/j.finel.2022.103866

[5] J.M.P. Martins, A. Andrade-Campos, S. Thuillier. Calibration of anisotropic plasticity models using a biaxial test and the virtual fields method, Int J Solids Struct 172–173 (2019) 21–37. https://doi.org/10.1016/j.ijsolstr.2019.05.019

[6] A. Maček, B. Starman, N. Mole, M. Halilovič. Calibration of advanced yield criteria using uniaxial and heterogeneous tensile test data, Metals 10 (2020). https://doi.org/10.3390/met10040542

[7] J.H. Kim, F. Barlat, F. Pierron, M.G. Lee. Determination of Anisotropic Plastic Constitutive Parameters Using the Virtual Fields Method, Exp Mech 54 (2014) 1189–204. https://doi.org/10.1007/s11340-014-9879-x

[8] M. Rossi, F. Pierron, M. Štamborská. Application of the virtual fields method to large strain anisotropic plasticity. Int J Solids Struct 97-98 (2016) 322–35. https://doi.org/10.1016/j.ijsolstr.2016.07.015

[9] S. Zhang, L. Léotoing, D. Guines, S. Thuillier, Potential of the cross biaxial test for anisotropy characterization based on heterogeneous strain field, Exp Mech 55 (2015) 817-835, https://doi.org/s11340-014-9983-y

[10] Y. Lou, S. Zhang, J.W. Yoon, Strength modeling of sheet metals from shear to plane strain tension, Int J Plast 134 (2020) 102813. https://doi.org/10.1016/j.ijplas.2020.102813

[11] J. Aquino, A. Andrade-Campos, J.M.P. Martins, S. Thuillier. Design of heterogeneous mechanical tests: Numerical methodology and experimental validation, Strain 55 (2019) 1–18. https://doi.org/10.1111/str.12313

[12] N. Souto, A. Andrade-Campos, S. Thuillier. A numerical methodology to design heterogeneous mechanical tests. Int J Mech Sci 107 (2016) 264–76. https://doi.org/10.1016/j.ijmecsci.2016.01.021

[13] M. Gonçalves, A. Andrade-Campos, B. Barroqueiro, On the design of mechanical heterogeneous specimens using multilevel topology optimization, Adv Eng Softw 175 (2023) 103314. https://doi.org/10.1016/j.advengsoft.2022.103314

[14] M. Gonçalves, A. Andrade-Campos, S. Thuillier, On the topology design of a mechanical heterogeneous specimen using geometric and material nonlinearities, IOP Conf. Ser.: Mater. Sci. Eng. 1238 (2022) 012055. https://doi.org/10.1088/1757-899x/1238/1/012055

[15] M. Grédiac, B. Blaysat, F. Sur. A Critical Comparison of Some Metrological Parameters Characterizing Local Digital Image Correlation and Grid Method, Exp Mech 57 (2017) 871–903. https://doi.org/10.1007/s11340-017-0279-x